

# A Memory-Based Approach to Model Glorious Uncertainties of Love

Aarsh Chotalia,\* Shiva Dixit,\* and P. Parmananda

Department of Physics, Indian Institute of Technology Bombay, Powai, Mumbai 400 076, India.

(Dated: August 17, 2023)

We propose a minimal yet intriguing model for a relationship between two individuals. The feeling of an individual is modeled by a complex variable and hence has two degrees of freedom [1]. The effect of memory of other individual's behavior in the past has now been incorporated via a conjugate coupling between each other's feelings. A region of parameter space exhibits multi-stable solutions wherein trajectories with different initial conditions end up in different aperiodic attractors. This aligns with the natural observation that most relationships are aperiodic and unique not only to themselves but, more importantly, to the initial conditions too. Thus, the inclusion of memory makes the task of predicting the trajectory of a relationship hopelessly impossible.

Human interactions can take place over a vast range of timescales. Of those, romantic relationships are the most intimate i.e. strongly coupled and generally long-standing. One approach to model such relations is to consider a dynamical system consisting of a large number of psychosomatic variables such as hormonal levels and employ neuropsychology-informed observations [2] to model the coupling and the effect of environment. Our approach in this work, however, is to consider a minimal model which is able to generate complex dynamics akin to what is observed in the real world.

Depending upon the nature of the coupling, a dynamical system may show a wide range of behaviors such as amplitude death, oscillation death, limit cycles, and chaos as the system parameters vary [3–7]. While modelling love dynamics has a long history starting from linear models [8, 9], there have been several recent attempts to model the dynamics of a romantic relationship with the inclusion of non-linearities [1, 10–13]. For a dynamist, the prime challenge is to quantify love as well as the coupling interaction between the lovers. Naturally, a sensible model must incorporate memory. The role of memory on affect has been discussed by psychologists[14]. The models in [11, 13] and [12, 15] have included memory effects using fractional ordered derivatives and time-delayed equations respectively. In this work, the effect of memory is encapsulated by a conjugate coupling [16–20] between the two lovers' feelings.

Typically, the variables in a dynamical systems are taken to be real numbers as they generally correspond to some real-world observable. A straightforward way to quantify feeling is to assign each of the two lovers a real number  $l_i$  ( $i = 1, 2$ ). The sign of  $l_i$  would determine whether the feeling is positive (i.e. love) or negative (i.e. hatred), while  $|l_i|$  would represent the intensity of the feeling. However, the types of behavior of dynamics are very limited for a two-dimensional phase space. Since we have two individuals, we must assign two real numbers to each lover. We, therefore, promote  $l_i$  to a complex number  $L_i \in \mathbb{C} \cong \mathbb{R}^2$  (henceforth referred to as “complex love”) of which real and imaginary parts are two real degrees of freedom making the phase space effectively

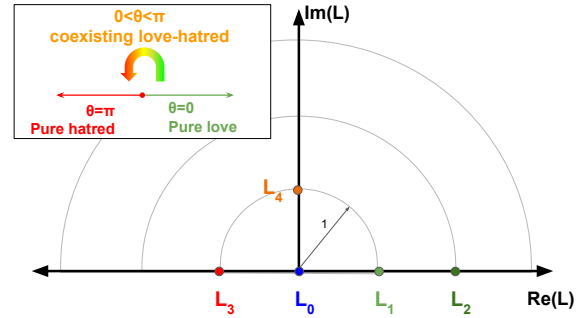


FIG. 1. (Color online) Love on the Argand plane: Interpretation of a complex love. The points  $L_0$  to  $L_4$  are examples of complex love.  $L_0 = 0 + 0i$ : apathy,  $L_1 = 1 + 0i$ : one unit pure love,  $L_2 = 2 + 0i$ : two units pure love,  $L_3 = -1 + 0i$ : one unit pure hatred and  $L_4 = 0 + i$ : coexisting half unit love and half unit hatred.

four-dimensional. This, as we shall see in the following paragraphs, makes the task of incorporating conjugate coupling easier and more natural.

The complex love number is to be interpreted in the following manner, which was first given by [1]. Love and hatred can coexist and the phase of the complex love determines the fraction of love. A phase of zero corresponds to a state of pure love while a phase of  $\pi$  corresponds to a state of pure hatred. Any intermediate phase  $\theta \in (0, \pi)$  would correspond to a state with co-existing love-hatred with a fraction of love  $f_l = \theta/\pi$  e.g. a phase of  $\pi/2$  would mean the person has an equal amount of love as hatred towards the other. Figure 1 shows some examples of possible complex loves. It should be noted that, under this interpretation, a complex love with a phase of  $\pi + \theta$  is to be considered equivalent to one with a phase of  $\pi - \theta$ .

While the time delay introduces coupling between the same variable at different times, conjugate coupling couples different variables at the same time. The latter serves as an indirect method to introduce a time delay without making the equations explicitly non-local in time. This accords with Takens' embedding theorem

[21] which states that a chaotic attractor may be reconstructed by using a time-delayed sequence of one component. The conjugate coupling has been used to capture time-delay by [20, 22, 23] in other settings. Mathematically, a dynamical system  $\{\mathbf{x}_1, \mathbf{x}_2, \dots, \mathbf{x}_n\}$  where each  $\mathbf{x}_i \in \mathbb{R}^m$  having a conjugate coupling evolves as

$$(\dot{\mathbf{x}}_i)_j = (\mathbf{f}_i(\mathbf{x}_i))_j + F_{ij}((\mathbf{x}_i)_j, (\mathbf{x}_k)_l) \quad (1)$$

where  $i, k = 1, \dots, n; j, l = 1, \dots, m; k \neq i; l \neq j$ .

In other words, the coupling term of the evolution of a given component of a given vector depends on itself and the complementary components of the other vectors. In particular, for a system of two 2-d vectors let  $j^{\text{th}}$  component of  $\mathbf{x}_i$  be  $x_{ij}$  where  $i, j = 1, 2$ , then  $x_{11}$  is coupled to  $x_{22}$  whereas  $x_{12}$  is coupled to  $x_{21}$  and vice-versa.

We name the two lovers ‘‘Layla’’ and ‘‘Majnun’’ after the central characters of the classic Persian love story ‘‘Layla-e-Majnun’’. Let  $L(t)$  ( $M(t)$ ) be the complex love Layla (Majnun) has for Majnun (Layla). The model given by Jafari et al. [1] for the temporal evolution of the relationship between Layla and Majnun is:

$$\frac{dL}{dt} = a + M^2 + c_1 L \quad (2)$$

$$\frac{dM}{dt} = b + L^2 + c_2 M \quad (3)$$

wherein the authors identify the parameters  $a$  and  $b$  as ‘‘environmental factors’’ for Majnun and Layla respectively. The environmental factor indicates the tendency of an individual to engage in a relationship due to their sociocultural environment. In the case of the Layla-Majnun story, in most versions, Layla is married to someone else, and therefore  $a$  is negative while Majnun is a young vagabond poet, looking for love, and therefore  $b$  is positive.

Our proposed model differs from the previous one in the final terms:

$$\frac{dL}{dt} = a + M^2 + c_1(L - iM) \quad (4)$$

$$\frac{dM}{dt} = b + L^2 + c_2(M - iL) \quad (5)$$

The final terms indicate the conjugate coupling between  $M$  and  $L$ . Note that when equations (4,5) are split into real and imaginary parts, the real part of  $L(M)$  gets coupled to the imaginary part of  $M(L)$  and vice-versa. As described earlier, this incorporates the memory of each other’s feelings in the past into the evolution of the relationship. For this reason, we term  $c_1$  and  $c_2$  as cross-memory parameters. One may easily deduce that the system is Hamiltonian if and only if  $c_1 + c_2 = 0$  with

$$H = bL - aM + \frac{ic}{2}(L^2 - M^2) - cML + \frac{L^3 - M^3}{3} \quad (6)$$

where  $c = c_1 = -c_2$ .

The fixed points of the system satisfy the following quartic equations:

$$L^4 - 2ic_2L^3 + (2b - c_2^2 + ic_1c_2)L^2 + (-2ibc_2 + 2c_1c_2^2)L + ac_2^2 + b^2 + ic_1c_2b = 0 \quad (7)$$

$$M^4 - 2ic_1M^3 + (2a - c_1^2 + ic_1c_2)M^2 + (-2iac_1 + 2c_1^2c_2)M + bc_1^2 + a^2 + ic_1c_2a = 0 \quad (8)$$

The Jacobian of (4,5) in the phase space  $(L_r, L_i, M_r, M_i)$ , where subscripts  $r$  and  $i$  denote the real and imaginary parts respectively, is given by:

$$J = \begin{bmatrix} c_1 & 0 & 2M_r & -2M_i + c_1 \\ 0 & c_1 & 2M_i - c_1 & 2M_r \\ 2L_r & -2L_i + c_2 & c_2 & 0 \\ 2L_i - c_2 & 2L_r & 0 & c_2 \end{bmatrix} \quad (9)$$

We simulated the equations (4,5) for different initial conditions as well as for different environmental factors and cross-memories using *MATLAB ver. R2021b* with the default differential equation solver *ode45*, which uses an optimum-adaptive step size. The initial conditions  $(L_r(0), L_i(0), M_r(0), M_i(0))$  were drawn uniformly from the interval  $[-1, 1]$ .

Firstly, we consider the case with fixed environmental factors ( $a = -1$  and  $b = 1$ ) and varying cross-memories  $c_1$  and  $c_2$  which are crucial model parameters that define the relationship. Our key interest is to identify the emergent collective dynamics due to the interplay of the cross memory strengths. Figure 2 (a) reveals a host of behaviours as the  $(c_1, c_2)$  space is traversed through  $[-1, 1] \times [-2, 2]$ . Noticeably, the  $c_1 = -c_2$  (white solid line) line on which the system is Hamiltonian also demarcates the regions of bound and unbound trajectories. The stability of the system can be understood from the eigenvalues of the Jacobian (equation 9) at the fixed points. Figure 2 (b) shows the largest (of four) real parts of the eigenvalues as  $c_1$  is varied from -1 to 1 keeping  $c_2 = -1.8$  fixed (white dashed line in Figure 2(i)). The two green intervals  $[-1, 0) \cup (0, 0.2)$  represent the values of  $c_1$  for which the system has a stable fixed point as  $Re(\lambda_{max})$  is negative in these intervals. At  $c_1 = 0$ , two solutions exchange their stabilities due to a transcritical bifurcation. When  $c_1$  approaches a value of about 0.2, the largest eigenvalue becomes positive and the stable solution, as shown in Figure 3 (iii), gives rise to stable limit cycle encircling a stable fixed point. This indicates to emergence of a supercritical Hopf bifurcation. Figure 2 (c) is the bifurcation diagram for  $L_r$  for the same range of  $c_1$ : The fixed stable point (red) bifurcates into multiple stable

limit cycles (green and blue) via a transcritical bifurcation at  $c_1 = 0$  before again becoming stable (red). At  $c_1 \approx 0.2$ , stable fixed point (red), through a supercritical Hopf bifurcation, gives rise to stable limit cycle (green) which in turn generates multiple limit cycles (blue) before reaching a region (cream) where multiple aperiodic trajectories corresponding to different initial conditions reside. As shown in Figure 2(a), once  $c_1$  exceeds  $-c_2$ , the basins for chaotic attractors vanish and all trajectories become unbounded (brown). This emphasises the need of having cross-memory since at  $(c_1, c_2) = (0, 0)$ , the system lives at the edge between multistable aperiodic attractors and the unbounded region. Similar bifurcations for varied  $c_2$  and fixed  $c_1$  have been presented in the supplementary material.

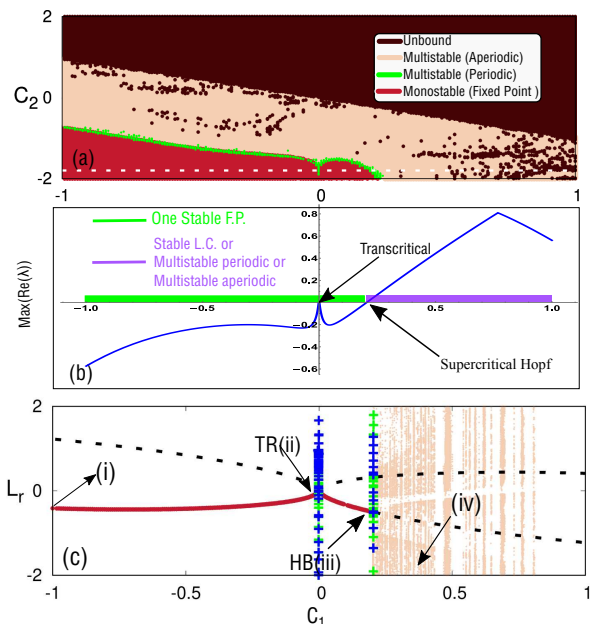


FIG. 2. (Color online) (a) The stability of the system in  $(c_1, c_2)$  plane: The environmental factors  $a$  and  $b$  are fixed to be  $-1$  and  $1$  respectively. The cream region is where multiple aperiodic orbits exist for different initial conditions. (b) Largest real part of eigenvalue of the Jacobian and (c) The bifurcation diagram produced using the software XPPAUT [24] as  $c_1$  is varied between  $-1$  and  $1$  at fixed  $c_2 = -1.8$  (i.e., along the white dashed horizontal line in (a)). For details see the text.

To illustrate the richness of the dynamics as cross-memory is varied, Figure 3 shows the time-series of  $L_r$  and the trajectories in the Layla plane (i.e.,  $L_r-L_i$  plane) for four different values of  $c_1$  in the bifurcation curve Figure 2 (c) i.e., with fixed  $(a, b, c_2) = (-1, +1, -1.8)$ . Each subfigure (i)-(iv) shows eight time-series and trajectories corresponding to eight different initial conditions having each of the four variables drawn uniformly at random from  $[-1, 1]$ . (i) At  $c_1 = -1$ , the system has a stable fixed

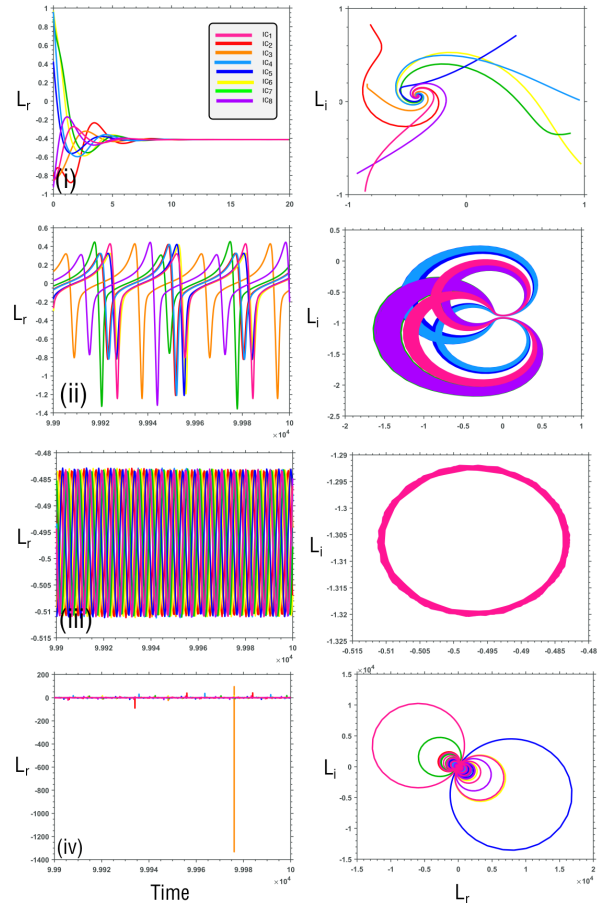


FIG. 3. (Color online) Time-series corresponding to Figure 2 (b) of  $L_r$  and the trajectories in the Layla plane (i.e.,  $L_r-L_i$  plane) for four different values of  $c_1 = (i) -1.0, (ii) 0.0, (iii) 0.2$  and  $(iv) 0.4$  with fixed  $(a, b, c_2) = (-1, +1, -1.8)$ . Each subfigure (i)-(iv) has time-series and trajectories corresponding to eight different initial conditions having each of the four variables drawn uniformly from  $[-1, 1]$ .

point  $(L_r^*, L_i^*, M_r^*, M_i^*) = (-0.41, 0.07, 0.58, -0.44)$ . (ii) At  $c_1 = 0$  and (iii)  $c_1 = 0.2$ , the system has multiple limit cycles and a single limit cycle, respectively. (iv) At  $c_1 = 0.4$  multiple aperiodic trajectories exist corresponding to different initial conditions. The periodic solutions reflect a typical stable relationship wherein the partners' emotions change slowly and predictably. On the contrary, the sporadic spikes in the aperiodic solutions are indicative of abrupt emotional fluctuations one experiences sometimes. A real life couple may indeed have time-dependent cross-memories that can lead to a solution that switches between periodic and aperiodic behaviour.

Finally, to understand how the external environment affects the dynamics, we varied the values of  $a$  and  $b$  between  $-2$  and  $2$ . As noted earlier, these environmental factors reflect the effect of socio-cultural environment on

an individual's tendency to love and thus serves as an overall bias in one's dynamics (equations 4,5). Figure 4 shows the dynamics of the system in the parameter space  $(a, b) \in [-2, 2] \times [-2, 2]$  with fixed cross-memories  $(c_1, c_2) = (0, -1.8)$ . Three types of behaviors are observed: stable fixed points (red), multistable aperiodic solutions (cyan), and unbounded solutions (brown).

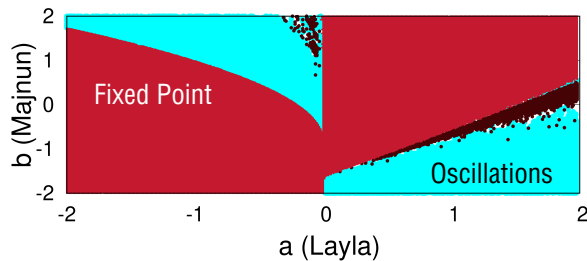


FIG. 4. (Color online) Effect of environmental factors  $a$  of Layla and  $b$  of Majnun with fixed cross-memories  $c_1 = 0$  and  $c_2 = -1.8$ . The red region has a stable fixed point while the cyan region exhibits multi-stable aperiodic solutions. In the black region, the system dynamics become unbounded for all initial conditions.

These results indicate that it is possible to obtain rich dynamics of human relationships just by considering a minimal model. Conjugate coupling serves to incorporate the effect of cross-memory without explicitly introducing time-delay, which is essential in understanding the system dynamics. Very interestingly, the parameter space contains regions wherein there are multiple chaotic attractors corresponding to different initial conditions. This type of multistability has been discussed in other settings by [25–27]. This is reminiscent of real-life scenarios: a relationship can not only be chaotic but also unique to itself for different initial conditions. A natural extension of this would be to consider a love triangle with three parties involved. These kinds of studies provide the basis for eventually understanding holistic social dynamics where the number of individuals and types of interaction is very large.

The unenviable and seemingly impossible task of capturing the dynamics of human emotions shows the hopelessness of prediction. It could be, on the other hand, considered the glorious uncertainties of love. The hope is that the interested readers would improve upon this model in a multidisciplinary fashion in an attempt to have a basic model that captures the human emotions at a nascent level.

\* These authors contributed equally to this work

- [1] S. Jafari, J. C. Sprott, and S. M. R. H. Golpayegani, *Nonlinear Dynamics* **83**, 615 (2016).
- [2] Z. Rubin, *Journal of personality and social psychology* **16**, 265 (1970).
- [3] W. Han, H. Cheng, Q. Dai, H. Li, P. Ju, and J. Yang, *Communications in Nonlinear Science and Numerical Simulation* **39**, 73 (2016).
- [4] K. Ponrasu, K. Sathiyadevi, V. Chandrasekar, and M. Lakshmanan, *Europhysics Letters* **124**, 20007 (2018).
- [5] A. Taher Azar, N. M. Adele, K. S. Tewa Alain, R. Kengne, and F. H. Bertrand, *Complexity* **2018**, 1 (2018).
- [6] M. F. Crowley and I. R. Epstein, *The Journal of Physical Chemistry* **93**, 2496 (1989).
- [7] E. Shajan, M. P. Asir, S. Dixit, J. Kurths, and M. D. Shrimali, *New Journal of Physics* **23**, 112001 (2021).
- [8] S. H. Strogatz, *Nonlinear dynamics and chaos with student solutions manual: With applications to physics, biology, chemistry, and engineering* (CRC press, 2018).
- [9] S. Rinaldi, *Applied Mathematics and Computation* **95**, 181 (1998).
- [10] K. M. Owolabi, *Physica A: Statistical Mechanics and its Applications* **525**, 849 (2019).
- [11] N. Ozalp and I. Koca, *Advances in Difference Equations* **2012**, 1 (2012).
- [12] W. Deng, X. Liao, T. Dong, and B. Zhou, *Neurocomputing* **260**, 13 (2017).
- [13] P. Kumar, V. S. Erturk, and M. Murillo-Arcila, *Chaos, Solitons & Fractals* **150**, 111091 (2021).
- [14] P. H. Blaney, *Psychological bulletin* **99**, 229 (1986).
- [15] N. Bielczyk, M. Bodnar, and U. Forys, *Applied Mathematics and Computation* **219**, 3923 (2012).
- [16] K. Yadav, N. Kamal, and M. Shrimali, *Physics Letters A* **383**, 2056 (2019).
- [17] T. Singla, N. Pawar, and P. Parmananda, *Physical review. E, Statistical, nonlinear, and soft matter physics* **83** **2 Pt 2**, 026210 (2011).
- [18] R. Karnatak, R. Ramaswamy, and A. Prasad, *Chaos: An Interdisciplinary Journal of Nonlinear Science* **19**, 033143 (2009).
- [19] K. Ponrasu, I. Gowthaman, V. Chandrasekar, and D. Senthilkumar, *Europhysics Letters* **128**, 58003 (2020).
- [20] R. Karnatak, R. Ramaswamy, and U. Feudel, *Chaos, Solitons & Fractals* **68**, 48 (2014).
- [21] F. Takens, in *Dynamical Systems and Turbulence, Warwick 1980*, edited by D. Rand and L.-S. Young (Springer Berlin Heidelberg, Berlin, Heidelberg, 1981) pp. 366–381.
- [22] M. M. Shrii, D. V. Senthilkumar, and J. Kurths, *Phys. Rev. E* **85**, 057203 (2012).
- [23] M. Dasgupta, M. Rivera, and P. Parmananda, *Chaos: An Interdisciplinary Journal of Nonlinear Science* **20** (2010).
- [24] B. Ermentrout, *Scholarpedia* **2**, 1399 (2007).
- [25] A. N. Pisarchik and U. Feudel, *Physics Reports* **540**, 167 (2014), control of multistability.
- [26] P. P. Singh and B. K. Roy, *Chaos, Solitons & Fractals* **161**, 112312 (2022).
- [27] K. Yadav, N. K. Kamal, and M. D. Shrimali, *Physical Review E* **95**, 042215 (2017).

# Supplementary Material For: A Memory-Based Approach to Model Glorious Uncertainties of Love

Aarsh Chotalia,\* Shiva Dixit,\* and P. Parmananda  
*Department of Physics, Indian Institute of Technology Bombay, Powai, Mumbai 400 076, India.*

## §-I. BIFURCATION ALONG $c_2$ AXIS

Figure SI-1 (a) shows the largest (of four) real parts of the eigenvalues as  $c_2$  is varied from -2 to 2 keeping  $c_1 = -0.5$  fixed. The green interval  $[-2, -1.21)$  represents the values of  $c_2$  for which the system has a stable fixed point as  $Re(\lambda_{max})$  is negative in these intervals. When  $c_1$  approaches a value of about 1.21, the largest eigenvalue becomes positive and the stable solution, as shown in Figure SI-1 (a), gives rise to stable limit cycle encircling a stable fixed point. This indicates to emergence of a supercritical Hopf bifurcation. Figure SI-1 (b) is the bifurcation diagram for  $L_r$  for the same range of  $c_2$ : At  $c_1 \approx -1.21$ , stable fixed point (red), through a supercritical Hopf bifurcation, gives rise to stable limit cycle (green) which in turn generates multiple limit cycles (blue) before reaching a region (cream) where multiple aperiodic trajectories corresponding to different initial conditions reside.

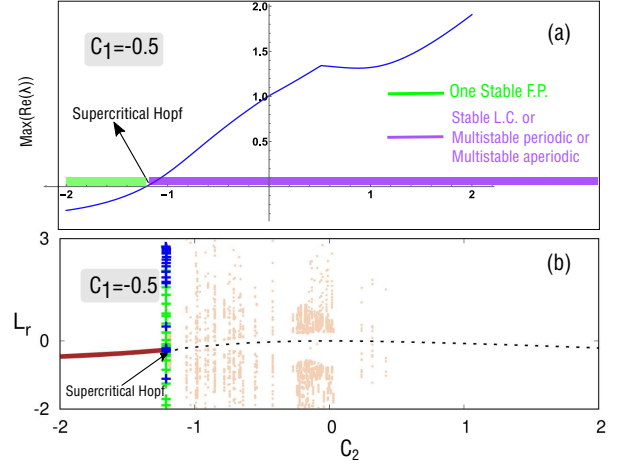


FIG. SI-1. (a) Largest real part of eigenvalue of the Jacobian and (b) The bifurcation diagram produced using the software XPPAUT as  $c_2$  is varied between -2 and 2 at fixed  $c_1 = -0.5$

\* These authors contributed equally to this work